A&A 606, A13 (2017)
DOI: 10.1051/0004-6361/201730726

Astronomy & Astrophysics

The High A_V Quasar Survey: A $z = 2.027$ metal-rich damped Lyman-α absorber towards a red quasar at $z = 3.21$⋆

J. P. U. Fynbo[1], J.-K. Krogager[1,2], K. E. Heintz[3,1], S. Geier[4,5], P. Møller[6], P. Noterdaeme[2], L. Christensen[1], C. Ledoux[7], and P. Jakobsson[3]

[1] Dark Cosmology Centre, Niels Bohr Institute, University of Copenhagen, Juliane Maries Vej 30, 2100 Copenhagen Ø, Denmark
e-mail: jfynbo@nbi.ku.dk
[2] Institut d'Astrophysique de Paris, CNRS-UPMC, UMR7095, 98bis bd Arago, 75014 Paris, France
[3] Centre for Astrophysics and Cosmology, Science Institute, University of Iceland, Dunhagi 5, 107 Reykjavík, Iceland
[4] Instituto de Astrofísica de Canarias, Vía Láctea, s/n, 38205 La Laguna, Tenerife, Spain
[5] Gran Telescopio Canarias (GRANTECAN), Cuesta de San José s/n, 38712 Breña Baja, La Palma, Spain
[6] European Southern Observatory, Karl-Schwarzschildstrasse 2, 85748 Garching, Germany
[7] European Southern Observatory, 3107 Alonso de Córdova, Casilla 19001, Vitacura, Santiago 19, Chile

Received 2 March 2017 / Accepted 21 June 2017

ABSTRACT

It is important to understand the selection effects behind the quasar samples to fully exploit the potential of quasars as probes of cosmic chemical evolution and the internal gas dynamics of galaxies; in particular, it is vital to understand whether the selection criteria exclude foreground galaxies with certain properties, most importantly a high dust content. Here we present spectroscopic follow-up from the 10.4 m GTC telescope of a dust-reddened quasar, eHAQ0111+0641, from the extended High A_V Quasar (HAQ) survey. We find that the $z = 3.21$ quasar has a foreground damped Lyman-α absorber (DLA) at $z = 2.027$ along the line of sight. The DLA has very strong metal lines due to a moderately high metallicity with an inferred lower limit of 25% of the solar metallicity, but a very large gas column density along the line of sight in its host galaxy. This discovery is further evidence that there is a dust bias affecting the census of metals, caused by the combined effect of dust obscuration and reddening, in existing samples of $z > 2$ DLAs. The case of eHAQ0111+0641 illustrates that dust bias is not only caused by dust obscuration, but also dust reddening.

Key words. quasars: general – quasars: absorption lines – quasars: individual: eHAQ0111+0641

1. Introduction

During the last two decades the study of the galaxy population of the first few Gyr after the Big Bang has undergone a revolution from a state with nearly no data to a state today with thousands of galaxies identified and studied in emission over a range of redshifts extending back to $z > 10$ (Madau & Dickinson 2014; Stark 2016). Prior to this revolution, galaxies at these early epochs were only studied in absorption against bright backlights such as quasars (Weymann et al. 1981). The damped Lyα absorbers (DLAs), which are Lyα absorbers with H I column densities above $10^{20.3}$ cm^{-2}, are of particular interest as they have all the properties expected for sightlines transversing the interstellar medium or, at least, circumgalactic material of actual galaxies (Wolfe et al. 1986, 2005).

Connecting the information inferred from studies of high redshift galaxies via absorption line studies and direct emission has not been straightforward. The so-called galaxy counterparts of the absorption selected systems, i.e. the shining components of the objects hosting the gas responsible for absorption line systems seen in quasar spectra, have long remained elusive to detect (e.g. Møller & Warren 1993; Djorgovski et al. 1996; Fynbo et al. 2010, and references therein).

A consistent picture is now emerging in which absorption, and here we specifically refer to DLAs, and emission studies of galaxies at $z > 2$ seem to probe the same underlying galaxy population in a way that to first order can be understood based on simple power-law scaling relations (evolving with redshift) between mass, luminosity, size, and metallicity (e.g. Fynbo et al. 1999, 2008; Haehnelt et al. 2000; Schaye 2001b; Møller et al. 2002, 2004, 2013; Ledoux et al. 2006; Krogager et al. 2012; Neeleman et al. 2013; Christensen et al. 2014; Krogager et al. 2017). In this picture the most metal-rich DLAs are formed in large and luminous galaxies, whereas the typical DLAs with lower metallicities are predominantly formed in much more numerous, but smaller and fainter dwarf galaxies. A good illustration of this is in Krogager et al. (2017, their Fig. 10). At least some hydro simulations of galaxies at these redshifts confirm this picture (Pontzen et al. 2008; Rahmati & Schaye 2014).

However, an important caveat to keep in mind is the issue of dust bias in the DLA samples. Metal-strong and DLAs that are, hence, likely to be dusty decrease the detection probability of the background quasars and hence such systems are under-represented in quasar samples selected in the optical. This effect has been discussed intensively in the literature (e.g. Ostriker & Heisler 1984; Pei et al. 1991, 1999; Boissé et al. 1998; Vladilo & Péroux 2005; Trenti & Stiavelli 2006; Pontzen & Pettini 2009; Wang et al. 2012).

Absorption statistics from radio selected samples of QSOs are free from dust bias as radio emission is not affected

⋆ The reduced spectrum (FITS file) is only available at the CDS via anonymous ftp to cdsarc.u-strasbg.fr (130.79.128.5) or via http://cdsarc.u-strasbg.fr/viz-bin/qcat?J/A+A/606/A13

by dust and *this* approach has been followed both in the CORALS survey (Ellison et al. 2001, 2005) and the UCSD survey (Jorgenson et al. 2006). The largest of those studies is the UCSD survey, which includes the CORALS data, but for which the optical identification is not complete. In this survey 26 DLAs have been identified, but Jorgenson et al. (2006) argue that a survey that is four times larger is needed to make a firm conclusion about the presence of a dust bias. Pontzen & Pettini (2009) argued that dust-bias is likely to be a small effect, but they found that the cosmic density of metals as measured from DLA surveys could be underestimated by as much as a factor of 2. Hence, further exploring and establishing the magnitude of the possible dust bias is important for the issue of cosmic chemical evolution.

The effect of dust that has been analysed in the context of DLAs and cosmic chemical evolution is that of obscuration of the light from the background quasar (e.g. Fall & Pei 1993; Boissé et al. 1998; Pei et al. 1999; Smette et al. 2005; Vladilo & Péroux 2005; Trenti & Stiavelli 2006; Pontzen & Pettini 2009). The other important effect of the dust is reddening, which also decreases the detection probability of the background quasar. Tentative evidence for this effect was found in a study of a metal-rich and dusty DLA in Fynbo et al. (2011). In this case the DLA moved the background quasar out to the edge of the colour distribution of the SDSS quasar locus and the DLA was only selected for spectroscopy because it fell into the selection window for high-z quasars because of its faint u-band flux. Several other quasars reddened by a foreground dusty absorbers have been found in SDSS, but again only because the strong reddening made the quasars fall into the selection window for very high redshift quasars or as filler objects for unused fibers (e.g. Noterdaeme et al. 2009; Wang et al. 2012; Pan et al. 2017).

Motivated by the object studied in Fynbo et al. (2011) the High A_V Quasar Survey (HAQ; Fynbo et al. 2013; Krogager et al. 2015, 2016a) for reddened quasars was initiated in 2011 with the objective of measuring the frequency of sources that are reddened out of the quasar selection criteria typically adopted in surveys such as SDSS (e.g. Schneider et al. 2010). In the HAQ survey we selected candidate quasars as point sources in regions of the sky with coverage at both optical and near-IR wavelengths, such as the overlapping regions of the Sloan Digital Sky Survey (SDSS) and UKIRT Infrared Deep Sky Survey (UKIDSS; Warren et al. 2007; Eisenstein et al. 2011). The HAQ survey has revealed a multitude of red quasars, but the large majority, more than 90%, of these quasars are red for other reasons than dust in foreground DLAs (see also Krawczyk et al. 2015; Zafar et al. 2015).

Krogager et al. (2016b) have presented the first clear case of a very bright quasar from the HAQ survey reddened by a $z > 2$ foreground, metal-rich, and dusty DLA. In this paper we present the second detection. eHAQ0111+0641 was selected from SDSS and UKIDSS imaging as part of the extended HAQ survey (Krogager et al. 2016a). In SDSS it is listed as an object of type "Star" based on its optical photometry. Its celestial coordinates are (J2000.0) RA = 01:11:34.7, Dec = +06:41:19.2. Krogager et al. (2016a) already noted this as a system where there is evidence for the 2175-Å dust extinction feature at a fitted redshift of 2.04 consistent within the errors with a strong metal-line system at $z = 2.027$.

The paper is organized in the following way: in Sect. 2 we present our new spectroscopic observations of eHAQ0111+0641. In Sect. 3 we present our results on the details of the DLA, constraints on its metallicity, and on the extinction. Finally we offer our conclusions in Sect. 4.

Table 1. Log of observations.

Date	Grism	Resolution	Exptime (s)	Airmass
11/09/2016	1000R	450	2×500	1.34–1.37
26/09/2016	1000B	500	3×1000	1.22–1.33
09/10/2016	2500U	1250	4×1800	1.11–1.08
19/01/2017	2500R	1850	3×720	1.32–1.43

2. Observations and data reduction

eHAQ0111+0641 was observed with the OSIRIS instrument at the Gran Telescopio Canarias (GTC) as part of a larger sample of candidate red quasars. We secured spectroscopy with OSIRIS and a range of grisms to better constrain the spectral energy distribution, metal lines, and hydrogen Lyα line. The log of observations is provided in Table 1.

The spectroscopic data were reduced using standard procedures in IRAF[1]. The spectra were flux calibrated with the observations of spectro-photometric standard stars observed on each of the nights of the corresponding science observations.

3. Results

In Fig. 1 we show the GTC spectra together with the photometry from SDSS, UKIDSS, and WISE. We also plot the composite quasar spectrum from Selsing et al. (2016) and a reddened version of this quasar composite. The overall shape of the spectrum is consistent with that found by Krogager et al. (2016a), i.e. with substantial reddening compared to the unreddened quasar composite.

Krogager et al. (2016a) found a $z = 2.027$ strong metal-line absorber in the lower resolution spectroscopy obtained at the Nordic Optical Telescope. Based on metal lines from Zn II, Cr II, and Fe II, in our 2500R spectrum we determine a more precise redshift of $z_{\rm abs} = 2.0273 \pm 0.0002$ for this system. At this redshift lines redward of about 1700 Å fall on the red side of the Lyα line of the quasar and hence outside of the Lyman forest.

3.1. Neutral hydrogen column density

The deep 2500U spectra covers the spectral region down to and blueward of the Lyα absorption line of the $z = 2.027$ system. This region is shown in the inset in the upper right-hand corner of Fig. 1. The H I column density is difficult to constrain precisely as the spectrum of the quasar is very reddened and as the line is on the blue side of the Lyman limit of the quasar. In the figure we have overplotted in red a model with a quasar composite spectrum that is reddened both by dust at the quasar redshift (SMC-like extinction at $z_{\rm quasar} = 3.214$, $A_V = 0.17 \pm 0.01$) and dust at the DLA redshift (LMC-like extinction at $z_{\rm DLA} = 2.027$, $A_V = 0.22 \pm 0.01$). The reddening was obtained by fitting the quasar template by Selsing et al. (2016) to the data using a combined dust model where dust is allowed to be both at the redshift of the absorber and the quasar. The fit is performed assuming SMC-type dust in the quasar and LMC-type dust in the absorber owing to the presence of the 2175 Å bump (for details on

[1] IRAF is distributed by the National Optical Astronomy Observatory, which is operated by the Association of Universities for Research in Astronomy (AURA) under a cooperative agreement with the National Science Foundation.

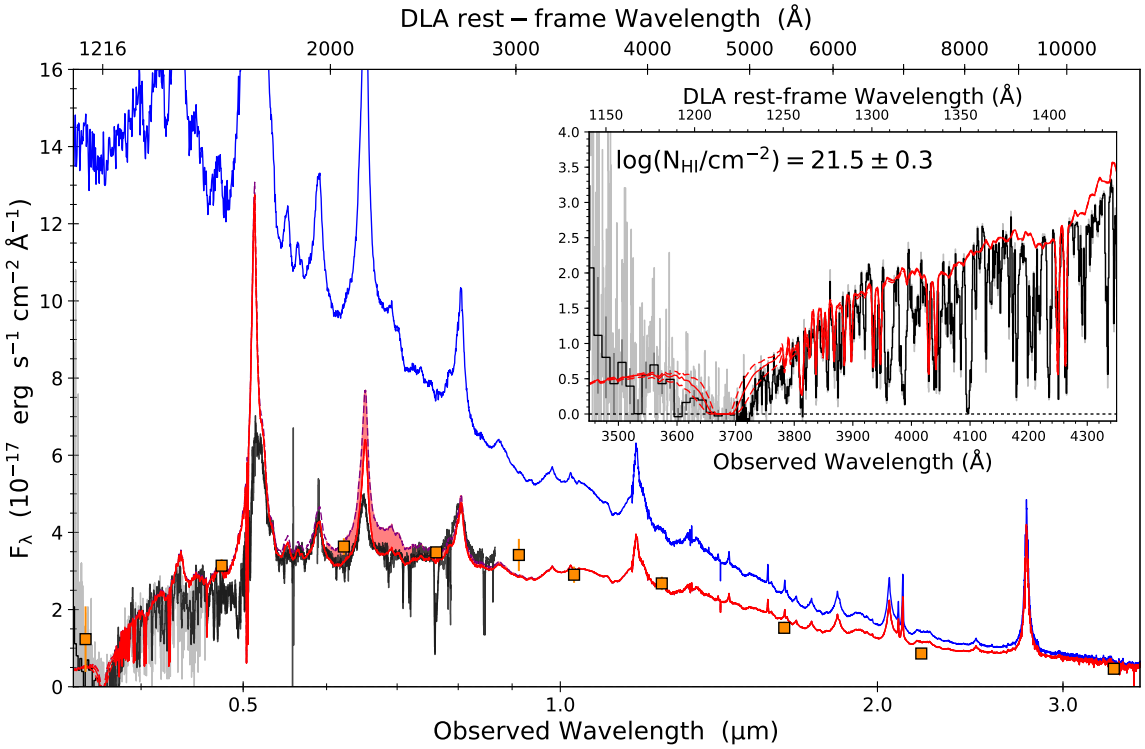

Fig. 1. GTC spectra shown together with the photometry from SDSS, UKIDSS, and WISE in the u, g, r, i, z, Y, JH, Ks, and W_1 bands (Warren et al. 2007; Wright et al. 2010; Eisenstein et al. 2011). We also overplot a composite quasar spectrum and a reddened composite as described in the text. The shaded area shows the effect of the 2175-Å extinction bump from dust in the $z = 2.027$ DLA galaxy. In the inset we plot a zoom on the blue part of the spectrum where we show the 2500U spectrum covering the region around the hydrogen Lyα line of the $z = 2.027$ absorber. Overplotted is the DLA fit assuming a column density of $10^{21.5\pm0.3}$ cm^{-2}; the $\pm1\sigma$ curves are shown with dashed lines.

this dual redshift dust fitting method see Krogager et al. (2015, 2016a)). The extinction curves used for the analysis are taken from the parametrization by Gordon et al. (2003). The statistical uncertainties from the fit on the derived A_V values is 0.01 mag, however, the uncertainty is dominated by systematic uncertainties because the intrinsic spectral shape of the template is not known a priori. This uncertainty is approximately 0.07 mag (Krogager et al. 2016b). The extinction curve for the absorber is shown in Fig. 2, where we isolated the dust contribution from the DLA. The quasar continuum model is very similar to the best fit derived from a formal fit to independent data from the Nordic Optical Telescope by Krogager et al. (2016a). We also included the effect of partial Lyman-limit absorption from two relatively strong Lyman-forest systems at $z = 3.1428$ and $z = 3.1555$, assuming column densities of $10^{16.4}$ cm^{-2} and $10^{16.6}$ cm^{-2}, respectively, to better model the continnum around the DLA line of the $z = 2.027$ absorber. Also included in the model are the Lyman lines from the two Lyman-limit systems (up to Lyman-31) and metal lines from S IIλ1250, 1253, 1259, Si IIλ1260, and Fe IIλ1260. For the $z = 2.027$ absorber we plotted curves for hydrogen column densities of $10^{21.5\pm0.3}$ cm^{-2} using the approximation of Tepper-García (2006, 2007). This model provides a reasonable fit to both the overall shape of the spectrum, photometry, and details of the region around the hydrogen line.

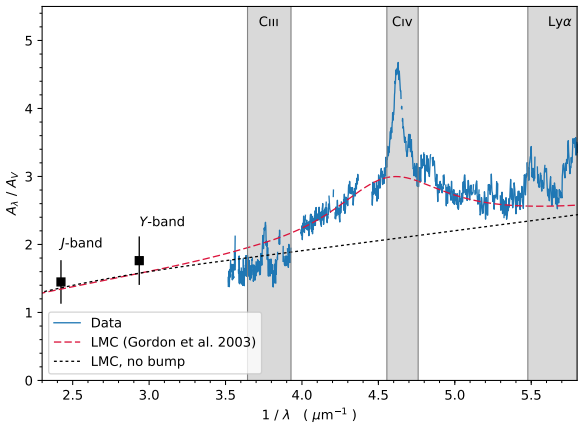

Fig. 2. Derived extinction curve from the dust in the absorber. The contribution from the quasar dust has been removed to highlight the 2175 Å dust bump from the absorber. The dashed line shows the LMC extinction curve by Gordon et al. (2003) and the dotted line shows the same extinction curve but with no bump. The position of emission lines is indicated by the shaded bands. Narrow peaks are caused by differences between the intrinsic quasar spectrum and the template used in the analysis.

3.2. Metallicity

The metal lines associated with the $z = 2.027$ absorber are very strong. In Table 2 we list the equivalent widths (EW) and column densities of all the detected absorption lines at the redshift of the DLA. As an example the rest-frame EW of the two components of the Mg II doublet are 2.8 and 2.6 Å, respectively. The redshift density of Mg II absorbers this strong or stronger is about 0.014 per co-moving path length based on the measurements in Seyffert et al. (2013). Compared to the DLAs in the very large sample of Noterdaeme et al. (2012), this DLA is among the 20% strongest Mg II absorbers.

Table 2. Subset of the absorption lines from the $z = 2.027$ DLA.

Ion	*EW* (rest) Å
Si II λ 1808	0.76 ± 0.07
Zn II, Mg I λ 2026	0.52 ± 0.05
Zn II λ 2026	0.39 ± 0.05
Cr II λ 2056	0.20 ± 0.04
Zn II, Cr II λ 2062	0.49 ± 0.05
Cr II λ 2066	0.18 ± 0.04
Fe II λ 2249	0.43 ± 0.03
Fe II λ 2260	0.44 ± 0.03
Fe II λ 2344	1.37 ± 0.04
Fe II λ 2374	1.17 ± 0.03
Fe II λ 2382	1.84 ± 0.03
Fe II λ 2586	1.20 ± 0.07
Fe II λ 2600	1.80 ± 0.05
Mg II λ 2796	2.72 ± 0.04
Mg II λ 2802	2.61 ± 0.04
Mg I λ 2852	1.24 ± 0.06

Notes. The Zn II λ 2026 EW was corrected for the contribution from Mg I λ 2026.

Table 3. Inferred column densities and metallicities from the DLA at $z = 2.027$ assuming a single component with fixed $b = 43$ km s^{-1}.

Element	log $N(X)$ (cm^{-2})	[X/H]$_\odot$
Fe	15.8 ± 0.1	−1.2 ± 0.3
Si	<16.7 ± 0.1	<−0.3 ± 0.3
Zn	13.5 ± 0.1	−0.6 ± 0.3
Cr	13.9 ± 0.1	−1.2 ± 0.3
Mg	13.6 ± 0.1	

The resolution of the 2500R grism with the 0.8 arcsec slit we used is $R = 1850$ around 6560 Å. We confirm this from measurements of the widths of sky lines. The seeing during the observations with the 2500R grism was above 1 arcsec and hence the resolution was set by the slit width. This resolution corresponds to 160 km s^{-1} in velocity space and this is too low to allow a proper Voigt-profile fit to the absorption lines. Instead we used the various Fe II lines available to constrain the curve of growth assuming a single component. This method can be assumed to provide at least a robust lower limit to the metallicity of the system (Prochaska 2006). This yields a best-fit b parameter of 43 ± 3 km s^{-1}. Assuming the same b parameter for all low-ion species, we can determine the abundances for other lines. The derived column densities are given in Table 3. The Si II λ 1808, line is surprisingly strong and we consider it likely that it is blended with an unidentified line. We hence consider the derived Si abundance an upper limit. The abundance of zinc is derived from the Zn II λ 2026 line, which is blended with Mg I. From the lower resolution 1000R spectrum, which covers the Mg I λ 2852 line, we can estimate the effect of the Mg I blend on Zn II. We constrain this to be 0.2 dex. This has been corrected in the column densities stated in Table 3.

In Fig. 3, we show the curve of growth (COG) derived for the Fe II lines. Assuming a constant b parameter for all other species, we show the other available species on the same COG. For species with only one transition available, the abundance is found by matching the equivalent width to the COG; that is why those points are observed to lie right on the COG.

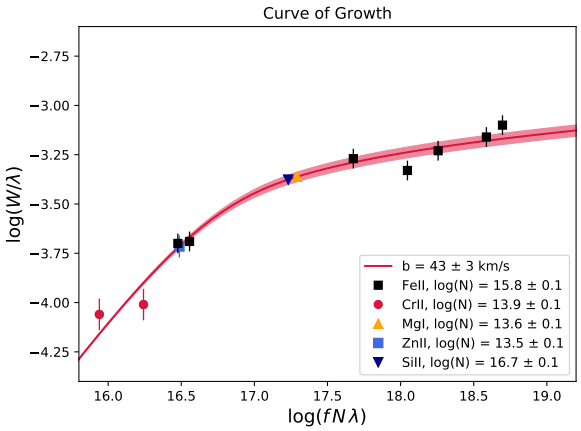

Fig. 3. Curve of growth (COG) for Fe II lines from the $z = 2.027$ DLA. The other species are assumed to follow the same COG and are plotted for comparison. The red shaded area indicates the 1σ uncertainty on the b parameter.

Based on the Zn measurement we can obtain the best estimate on the overall metallicity of the system because most of the Zn should be in the gas phase (Pettini et al. 1997a,b). Using solar abundances from Asplund et al. (2009), we infer a Zn metallicity lower limit of −0.6 ± 0.3. The [Cr/Zn] and [Fe/Zn] ratios taken at face value are both −0.6 ± 0.1, which following the relations between metallicity and depletion in De Cia et al. (2016) corresponds to a metallicity of −1.0. This is at least consistent in case the derived column densities are close to the true values.

3.3. Extinction

It is not possible to derive the precise amount of extinction and the corresponding extinction curve unambiguously. To do this requires assumptions about the shape of the underlying quasar spectrum. The majority of bright quasars, however, do appear to have remarkably similar spectra. This is for example illustrated by the fact that several independent composite spectra agree well with each other (e.g. Selsing et al. 2016).

In the case of eHAQ0111+0641 Krogager et al. (2016a) assumed that the underlying, intrinsic spectrum of eHAQ0111+0641 is similar to the composite spectrum of Selsing et al. (2016). They found that the spectrum was best modelled by the composite spectrum reddened by dust both intrinsic to the quasar host galaxy and the $z = 2.027$ intervening absorber. Krogager et al. also found evidence of the presence of the 2175-Å dust extinction feature. This somewhat elusive dust feature is well known from the Milky Way, present in the LMC, and largely missing in extinction curves probed in the SMC. It has been detected in some $z > 1$ gamma-ray burst and quasar sightlines (e.g. Junkkarinen et al. 2004; Srianand et al. 2008; Elíasdóttir et al. 2009; Prochaska et al. 2009; Noterdaeme et al. 2009; Conroy et al. 2010; Jiang et al. 2011; Kulkarni et al. 2011; Zafar et al. 2012; Ma et al. 2015; Ledoux et al. 2015).

In Fig. 1 we show that the model derived by Krogager et al. (2016a) provides a very good match to our spectra, including the 2175-Å extinction feature illustrated with the shaded area.

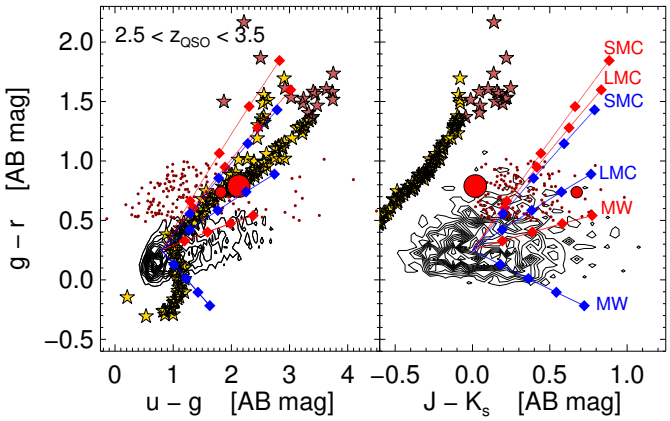

Fig. 4. Colour-colour distributions of the SDSS/BOSS-DR12 quasar sample in the redshift range, $2.5 < z < 3.5$ (black contours). The reddening has moved eHAQ0111+0641 (shown with a large red circle) away from the quasar locus onto the stellar track indicated with yellow (normal stars) and red (M-dwarfs and later) stars. The small red circle shows the position of HAQ2225+0527 discussed in Krogager et al. (2016a), which also falls on the stellar track in the SDSS colours. In the near-IR the object is well separated from the stellar track. The dark red points show the distribution of 150 HAQs from Krogager et al. (2015). Also plotted are the reddening vectors for a $z = 3$ quasar reddened by SMC, LMC, and MW extinction curves from Pei (1992) at foreground redshifts of 2.0 (blue lines) and 2.5 (red lines). The diamonds along the lines show the points corresponding to A_Vs of 0.5, 1.0, 1.5, and 2.0.

3.4. Emission from the galaxy counterpart

We find no evidence for emission lines from the galaxy counterpart of the DLA. The only line our spectroscopy allows us to detect is the Lyα emission line and that is not detected in our 2500U grism observation down to a 3σ flux limit of 5×10^{-17} erg s^{-1} cm^{-2}. This corresponds to a star formation rate of 1.5 $M_\odot$ yr^{-1} following the calculation in Fynbo et al. (2002). This non-detection is not surprising given that we only have one slit position and given that Ly-α emission can often be very weak even for strongly star-forming DLA galaxy counterparts (e.g. Fynbo et al. 2011; Krogager et al. 2017).

The target would be very interesting for a follow-up study in the near-IR that would allow detection of the rest-frame optical emission lines, such as [O II], [O III], and Balmer lines.

4. Discussion and conclusions

In Fig. 4 we show $g - r$ versus $u - g$ and $J - K_s$ colour-colour (on the AB magnitude system) plots of quasars from the SDSS/Baryon Oscillation Spectroscopic Survey (BOSS) data release (DR) 12 (Eisenstein et al. 2011) and the colours of normal stars and cool dwarfs from Hewett et al. (2006). The plot illustrates the effect of reddening on the quasar selection probability. In the optical the reddening has moved eHAQ0111+0641 away from the quasar locus onto the stellar track. In the near-IR, however, the object is clearly separated from the stellar track owing to the redder near-IR emission given its $g - r$ colour.

Three points are remarkable. First, the quasar is relatively bright (with an AB magnitude of 18.55 ± 0.01 in the UKIDSS K_s band), which illustrates that also bright quasars can evade selection. This point was even more clearly illustrated in the case of HAQ2225+0527 (Krogager et al. 2016b), where the quasar was very bright at $K_s = 16.15 \pm 0.01$ and still evaded selection in the SDSS/BOSS surveys. This quasar, however, was previously detected as a bright radio source. Also the quasar studied by Wang et al. (2012) is intrinsically very bright. Second, the amount of reddening that is sufficient to remove these objects from the selection windows is very small – just a few tenths of a magnitude in the DLA rest-frame V-band. And third, the metallicity of the absorber, although it is just a lower limit, is not very large at around 25% solar. In the case of HAQ2225+0527 the metallicity was higher, around solar, but the H I column density was in this case smaller such that the amount of absorption was similar, i.e. a few tenths of a magnitude *dust extinction* in the DLA rest-frame V band. Boissé et al. (1998) found that the upper envelope of DLAs in the metallicity versus H I column density plot corresponds to a few tenths of a magnitude dust extinction in the DLA rest-frame V band. This is consistent with the findings of Heintz et al. (2016, see also Barkhouse & Hall 2001; Glikman et al. 2013), namely that only half of the HAQ quasars in the COSMOS field were picked up by the SDSS/BOSS quasar survey despite only modest amounts of reddening.

The few cases of DLAs causing reddening of their background quasars just straddle this envelope noticed by Boissé et al. (1998), but there are good reasons to think that there are systems further above this apparent demarcation line. From spectroscopic studies of gamma-ray burst afterglows we know of several systems with significantly higher extinction in the rest-frame V band and with relatively high metallicities, for example the case of GRB 080607 (Prochaska et al. 2009) or GRB 050401 (Watson et al. 2006). Krühler et al. (2013) have argued that these systems probably are more common among GRB absorbers than inferred from the samples of well-observed optical afterglow due to dust bias (see also Fynbo et al. 2009, who find evidence for dust bias in the sample of GRBs with detected optical afterglows). The reduced number of absorbers above the Boissé-line may be partly caused by the conversion of H I to molecular hydrogen (Schaye 2001a; Krumholz et al. 2009).

DLAs are a crucial class of objects in the reconstruction of the cosmic chemical enrichment history (e.g. Pettini et al. 1994; Lu et al. 1996; Prochaska et al. 2003; Rafelski et al. 2014; Ledoux et al. 2015). Pontzen & Pettini (2009) find that the cosmic density of metals as measured from DLA surveys could be underestimated by as much as a factor of 2 owing to dust obscuration, and with the added effect of dust reddening this effect could certainly be larger, although not dramatically larger. This is something we will try to quantify in a future paper. To identify more metal-rich, and hence, more dusty DLAs towards quasar sightlines, and hence obtain a more representative sample from which to derive the cosmic chemical enrichment history, we need to target redder (in $J - K_s$) and most likely optically fainter quasars as well. In Fig. 4 we also show colour tracks for a $z = 3$ quasar spectrum reddened by extinction curves representative for the SMC, LMC, and MW from Pei (1992) with A_V ranging from 0 to 2 (values at $A_V = 0.5$, 1., 1.5, and 2.0 are indicated with diamonds) and for assumed DLA redshifts of 2.5 (red lines) and 2.0 (blue lines). It is interesting that MW-type extinction, due to the 2175 Å extinction feature falling in the r band, makes the quasars bluer in $g - r$ if the DLA is at $z \approx 2$. Such quasars ought to be relatively easy to identify (see also Wang et al. 2004; Ledoux et al. 2015).

In addition to reddening the extinction of course makes the quasars fainter as well. The upcoming EUCLID legacy survey will be a promising starting point for such a target selection. It is already clear that the population of reddened quasars is significant in terms of numbers. Heintz et al. (2016) have found from their study of a complete sample of quasars in the COSMOS field that at magnitude limit of $J < 20$ about 20% of quasars are reddened at a level corresponding to $E(B - V) > 0.1$. Most

likely only a few percent of these quasars are red because of foreground DLAs, but in terms of metals this may still be an important contribution. In a future paper we plan to make a quantitative analysis of the magnitude and implication of the dust bias, including the effects of both obscuration and reddening, on the measurement of the cosmic abundance of metals in galaxies. For now we conclude that objects, such as eHAQ0111+0641 and HAQ2225+0527, provide positive evidence that there is a dust bias against metal-rich DLAs in existing samples of $z > 2$ DLAs and that, using existing samples, we hence must to some extent be underestimating the cosmic abundances of metals in DLAs.

Acknowledgements. Based on observations made with the Gran Telescopio Canarias (GTC), installed at the Spanish Observatorio del Roque de los Muchachos of the Instituto de Astrofísica de Canarias on the island of La Palma. The research leading to these results has received funding from the European Research Council under the European Union's Seventh Framework Programme (FP7/2007-2013)/ERC Grant agreement no. EGGS-278202. J.K. acknowledges financial support from the Danish Council for Independent Research (EU-FP7 under the Marie-Curie grant agreement no. 600207) with reference DFF-MOBILEX–5051-00115. K.E.H. and P.J. acknowledge support by a Project Grant (162948–051) from The Icelandic Research Fund. P.N. acknowledges support from the Programme National de Cosmologie et Galaxies (PNCG) funded by CNRS/INSU-IN2P3-INP, CEA, and CNES, France.

References

Asplund, M., Grevesse, N., Sauval, A. J., & Scott, P. 2009, ARA&A, 47, 481
Barkhouse, W. A., & Hall, P. B. 2001, AJ, 121, 2843
Boissé, P., Le Brun, V., Bergeron, J., & Deharveng, J.-M. 1998, A&A, 333, 841
Christensen, L., Møller, P., Fynbo, J. P. U., & Zafar, T. 2014, MNRAS, 445, 225
Conroy, C., Schiminovich, D., & Blanton, M. R. 2010, ApJ, 718, 184
De Cia, A., Ledoux, C., Mattsson, L., et al. 2016, A&A, 596, A97
Djorgovski, S. G., Pahre, M. A., Bechtold, J., & Elston, R. 1996, Nature, 382, 234
Eisenstein, D. J., Weinberg, D. H., Agol, E., et al. 2011, AJ, 142, 72
Elíasdóttir, Á., Fynbo, J. P. U., Hjorth, J., et al. 2009, ApJ, 697, 1725
Ellison, S. L., Yan, L., Hook, I. M., et al. 2001, A&A, 379, 393
Ellison, S. L., Hall, P. B., & Lira, P. 2005, AJ, 130, 1345
Fynbo, J. P. U., Prochaska, J. X., Sommer-Larsen, J., Dessauges-Zavadsky, M., & Møller, P. 2008, ApJ, 683, 321
Fall, S. M., & Pei, Y. C. 1993, ApJ, 402, 479
Fynbo, J. U., Møller, P., & Warren, S. J. 1999, MNRAS, 305, 849
Fynbo, J. P. U., Møller, P., Thomsen, B., et al. 2002, A&A, 388, 425
Fynbo, J. P. U., Jakobsson, P., Prochaska, J. X., et al. 2009, ApJS, 185, 526
Fynbo, J. P. U., Laursen, P., Ledoux, C., et al. 2010, MNRAS, 408, 2128
Fynbo, J. P. U., Ledoux, C., Noterdaeme, P., et al. 2011, MNRAS, 413, 2481
Fynbo, J. P. U., Krogager, J.-K., Venemans, B., et al. 2013, ApJS, 204, 6
Glikman, E., Urrutia, T., Lacy, M., et al. 2013, ApJ, 778, 127
Gordon, K. D., Clayton, G. C., Misselt, K. A., Landolt, A. U., & Wolff, M. J. 2003, ApJ, 594, 279
Haehnelt, M. G., Steinmetz, M., & Rauch, M. 2000, ApJ, 534, 594
Heintz, K. E., Fynbo, J. P. U., Møller, P., et al. 2016, A&A, 595, A13
Hewett, P. C., Warren, S. J., Leggett, S. K., & Hodgkin, S. T. 2006, MNRAS, 367, 454
Jiang, P., Ge, J., Zhou, H., Wang, J., & Wang, T. 2011, ApJ, 732, 110
Jorgenson, R. A., Wolfe, A. M., Prochaska, J. X., et al. 2006, ApJ, 646, 730
Junkkarinen, V. T., Cohen, R. D., Beaver, E. A., et al. 2004, ApJ, 614, 658
Krawczyk, C. M., Richards, G. T., Gallagher, S. C., et al. 2015, AJ, 149, 203
Krogager, J.-K., Fynbo, J. P. U., Møller, P., et al. 2012, MNRAS, 424, L1
Krogager, J.-K., Geier, S., Fynbo, J. P. U., et al. 2015, ApJS, 217, 5
Krogager, J.-K., Fynbo, J. P. U., Heintz, K. E., et al. 2016a, ApJ, 832, 49
Krogager, J.-K., Fynbo, J. P. U., Noterdaeme, P., et al. 2016b, MNRAS, 455, 2698
Krogager, J.-K., Møller, P., Fynbo, J. P. U., & Noterdaeme, P. 2017, MNRAS, 469, 2959
Krühler, T., Ledoux, C., Fynbo, J. P. U., et al. 2013, A&A, 557, A18
Krumholz, M. R., Ellison, S. L., Prochaska, J. X., & Tumlinson, J. 2009, ApJ, 701, L12
Kulkarni, V. P., Torres-Garcia, L. M., Som, D., et al. 2011, ApJ, 726, 14
Ledoux, C., Petitjean, P., Fynbo, J. P. U., Møller, P., & Srianand, R. 2006, A&A, 457, 71
Ledoux, C., Noterdaeme, P., Petitjean, P., & Srianand, R. 2015, A&A, 580, A8
Lu, L., Sargent, W. L. W., Barlow, T. A., Churchill, C. W., & Vogt, S. S. 1996, ApJS, 107, 475
Ma, J., Caucal, P., Noterdaeme, P., et al. 2015, MNRAS, 454, 1751
Madau, P., & Dickinson, M. 2014, ARA&A, 52, 415
Møller, P., & Warren, S. J. 1993, A&A, 270, 43
Møller, P., Warren, S. J., Fall, S. M., Fynbo, J. U., & Jakobsen, P. 2002, ApJ, 574, 51
Møller, P., Fynbo, J. P. U., & Fall, S. M. 2004, A&A, 422, L33
Møller, P., Fynbo, J. P. U., Ledoux, C., & Nilsson, K. K. 2013, MNRAS, 430, 2680
Neeleman, M., Wolfe, A. M., Prochaska, J. X., & Rafelski, M. 2013, ApJ, 769, 54
Noterdaeme, P., Ledoux, C., Srianand, R., Petitjean, P., & Lopez, S. 2009, A&A, 503, 765
Noterdaeme, P., Petitjean, P., Carithers, W. C., et al. 2012, A&A, 547, L1
Ostriker, J. P., & Heisler, J. 1984, ApJ, 278, 1
Pan, X., Zhou, H., Ge, J., et al. 2017, ApJ, 835, 218
Pei, Y. C. 1992, ApJ, 395, 130
Pei, Y. C., Fall, S. M., & Bechtold, J. 1991, ApJ, 378, 6
Pei, Y. C., Fall, S. M., & Hauser, M. G. 1999, ApJ, 522, 604
Pettini, M., Smith, L. J., Hunstead, R. W., & King, D. L. 1994, ApJ, 426, 79
Pettini, M., King, D. L., Smith, L. J., & Hunstead, R. W. 1997a, ApJ, 478, 536
Pettini, M., Smith, L. J., King, D. L., & Hunstead, R. W. 1997b, ApJ, 486, 665
Pontzen, A., & Pettini, M. 2009, MNRAS, 393, 557
Pontzen, A., Governato, F., Pettini, M., et al. 2008, MNRAS, 390, 1349
Prochaska, J. X. 2006, ApJ, 650, 272
Prochaska, J. X., Gawiser, E., Wolfe, A. M., Castro, S., & Djorgovski, S. G. 2003, ApJ, 595, L9
Prochaska, J. X., Sheffer, Y., Perley, D. A., et al. 2009, ApJ, 691, L27
Rafelski, M., Neeleman, M., Fumagalli, M., Wolfe, A. M., & Prochaska, J. X. 2014, ApJ, 782, L29
Rahmati, A., & Schaye, J. 2014, MNRAS, 438, 529
Schaye, J. 2001a, ApJ, 562, L95
Schaye, J. 2001b, ApJ, 559, L1
Schneider, D. P., Richards, G. T., Hall, P. B., et al. 2010, AJ, 139, 2360
Selsing, J., Fynbo, J. P. U., Christensen, L., & Krogager, J.-K. 2016, A&A, 585, A87
Seyffert, E. N., Cooksey, K. L., Simcoe, R. A., et al. 2013, ApJ, 779, 161
Smette, A., Wisotzki, L., Ledoux, C., et al. 2005, in Probing Galaxies through Quasar Absorption Lines, eds. P. Williams, C.-G. Shu, & B. Menard, IAU Colloq., 199, 475
Srianand, R., Gupta, N., Petitjean, P., Noterdaeme, P., & Saikia, D. J. 2008, MNRAS, 391, L69
Stark, D. P. 2016, ARA&A, 54, 761
Tepper-García, T. 2006, MNRAS, 369, 2025
Tepper-García, T. 2007, MNRAS, 382, 1375
Trenti, M., & Stiavelli, M. 2006, ApJ, 651, 51
Vladilo, G., & Péroux, C. 2005, A&A, 444, 461
Wang, J., Hall, P. B., Ge, J., Li, A., & Schneider, D. P. 2004, ApJ, 609, 589
Wang, J.-G., Zhou, H.-Y., Ge, J., et al. 2012, ApJ, 760, 42
Warren, S. J., Hambly, N. C., Dye, S., et al. 2007, MNRAS, 375, 213
Watson, D., Fynbo, J. P. U., Ledoux, C., et al. 2006, ApJ, 652, 1011
Weymann, R. J., Carswell, R. F., & Smith, M. G. 1981, ARA&A, 19, 41
Wolfe, A. M., Turnshek, D. A., Smith, H. E., & Cohen, R. D. 1986, ApJS, 61, 249
Wolfe, A. M., Gawiser, E., & Prochaska, J. X. 2005, ARA&A, 43, 861
Wright, E. L., Eisenhardt, P. R. M., Mainzer, A. K., et al. 2010, AJ, 140, 1868
Zafar, T., Watson, D., Elíasdóttir, Á., et al. 2012, ApJ, 753, 82
Zafar, T., Møller, P., Watson, D., et al. 2015, A&A, 584, A100